Aalborg Universitet

AALBORG UNIVERSITY
DENMARK

Radio Propagation Analysis of Industrial Scenarios within the Context of Ultra-Reliable Communication

Wassie, Dereje Assefa ; Rodriguez Larrad, Ignacio; Berardinelli, Gilberto; Tavares, Fernando Menezes Leitão; Sørensen, Troels Bundgaard; Mogensen, Preben Elgaard

Publication date:
2018

Document Version
Accepted author manuscript, peer reviewed version

Link to publication from Aalborg University

Radio Propagation Analysis of Industrial Scenarios within the Context of Ultra-Reliable Communication

Dereje Assefa Wassie [(1)], Ignacio Rodriguez [(1)], Gilberto Berardinelli [(1)], Fernando M. L. Tavares [(1)],
Troels B. Sørensen [(1)], Preben Mogensen [(1),(2)]

[(1)] Department of Electronic Systems, Aalborg University, Denmark
[(2)] Nokia Bell Labs, Aalborg, Denmark
E-mail: {daw, irl, gb, ft, tbs, pm}@es.aau.dk

Abstract—One of the 5G use cases, known as ultra-reliable communication (URC), is expected to support very low packet error rate on the order of 10^{-5} with a 1 ms latency. In an industrial scenario, this would make possible replacing wired connections with wireless for controlling critical processes. Industrial environments with large metallic machinery and concrete structures can lead to deep shadowing and severe fading in the radio propagation channel, and thus pose a challenge for achieving the outage levels in connection with URC. In this paper, we present and analyze the large-scale propagation characteristics of two different industrial environments - open production space and dense factory clutter - based on measurements conducted at 2.3 and 5.7 GHz

By including a large number of spatially distributed samples, as per our experimental approach, we show the importance of properly characterizing the large-scale fading outage for URC. For instance, we show that based on a simple one-slope distance dependent path loss model, the conventional log-normal model for large-scale shadow fading is by far too simple for this environment. Our results show that at the 10^{-4} percentile, the tail of the shadow fading distribution can deviate by up to 10-20 dB from the log-normal model with respect to the average NLOS values (around 6 dB and 8 dB at 2.3 and 5.7 GHz, respectively). The simplicity of the one-slope path loss model, and its ability as we show, to express the trends with respect to scenarios, frequencies, and antenna heights, makes it an attractable option. However, there is a need for further experimental insight, possibly in combination with deterministic analysis, to get a better understanding of the large-scale fading for the study of URC in industrial environments.

Index Terms—Ultra-reliable communication, 5G, propagation, industrial, path loss.

I. INTRODUCTION

One of the key features of the 5G wireless communication system is the support of new mission-critical applications which demand high reliability, known as ultra-reliable communication. Most of ultra-reliability communication services require 99.999% reliability and usually very low latency [1]. Furthermore, ultra-reliable communication opens a wide range of use cases, such as industry automation, vehicular communication for traffic safety/control, and energy management.

With respect to industry automation, ultra-reliable communication enables a significant benefit on monitoring and controlling the physical process of the industry, such as assembly lines and logistics, by offering a more flexible communication infrastructure compared with the existing wired

communication. However, there are many challenges to be addressed for verifying the potential of ultra-reliable communication in an industrial environment, such as the radio propagation conditions. The radio propagation conditions in large industrial buildings are expected to be severe due to concrete structure and presence of large metallic machinery. This condition may affect the spatial availability of the wireless communication signal. In that respect, extensive radio propagation measurements are crucial to understand the radio channel characteristics in the context of ultra-reliable communication in such environments. Particularly for this context, one needs to understand the occurrence and characteristics of severe fading, which is commonly expressed in the tails of the shadow fading distributions. A considerable effort on the measurement campaign is therefore needed to ensure a large number of measurement samples over multiple locations, containing representative information about the diverse radio propagation possibilities in the environment.

Limited works have been done on characterizing the radio propagation aspects of the industrial environments. The work in [2] investigated the large-scale radio propagation characteristics at a frequency of 1.3 GHz in different factories like food processing, engine factory, and aluminum manufacturing. The measurements were performed at three measurement locations in each factory where the transmitter and receiver separation range was between 10 m and 80 m and the transmitter/receiver antennas were 2 m above the ground. A similar narrow-band study was also executed at a carrier frequency of 2.4 GHz in a chemical pulp factory, a cable production hall, and a nuclear power plant [3]. The measurements were executed along two measurement routes with a maximum distance of 95 m. The work in [4] also explored the propagation characteristics in a nuclear power plant environment with the measurements being executed at nine positions with a maximum transmitter and receiver separation distance of 13 m. In [5] propagation measurements were carried out at frequencies of 900 MHz, 2.4 GHz, and 5.2 GHz in wood and metal processing factories. The measurements were performed with a transmitter antenna height of 6 m and receiver antenna height of 2 m with a maximum distance of 140 m in between, and a different number of path-loss samples were also collected for the three frequencies. The work in [6] investigated different empirical

path loss models for industrial environment radio coverage by measuring the received signal strength indicator (RSSI) of the beacon frame transmitted by IEEE802.11a/b/g access points. The measurements were conducted along two measurement routes using two access points installed at 2 m and 4.85 m with the receiver being at 1 m above the ground. Measurements spanning over a large frequency band 200-2500 MHz were also carried out in an industrial environment [7] where the transmitter/receiver antennas were mounted 1 m above the floor. The measurements included 1601 measurement points with a maximum distance of 18 m between the transmitter and receiver locations. In addition, large-scale radio propagation in the civil engineering laboratory, which consists soft and hard structure besides machinery, was also investigated in [8] at a frequency of 2.4 GHz with a 36 path loss samples, where the transmitter was mounted at three different heights like 1.5 m, 2 m, and 3 m and the receiver installed only at 1.71 m above the floor.

In most of aforementioned works, the spatial measurement coverage over a given industrial environment was restricted, and had relatively low number of representative measurement points (in the order of tenths to few thousands). In addition, most of the measurements were carried out over specific measurement routes on a limited set of locations; with the objective to characterize the tails of the distribution, viz ultra-reliable communication, this is likely insufficient.

This paper presents an empirical analysis of wideband large-scale radio propagation in two industrial scenarios at 2.3 GHz and 5.7 GHz. Compared to previous studies, extensive measurement campaigns are performed for obtaining a total of 8,832 wideband path loss measurement samples per frequency and scenario. The measurements are conducted at 24 uniformly spatial-distributed locations in each scenario for multiple antenna configurations considering all possible link combinations between two different heights: 0.25 and 1.75 m. Our measurement approach allows better spatial coverage of the environments, facilitating, at least, a partial characterization of the tails of the shadowing distributions.

The rest of the paper is organized as follows. In Section II, the measurement setup and industrial scenarios are introduced. Section III discusses the wideband large-scale propagation measurement results and derived models, and presents the results in the perspective of ultra-reliable communication. Finally, the conclusion of the study is drawn in Section IV.

II. MEASUREMENT SETUP AND SCENARIOS

A. Industrial Scenarios

Two industrial production lab facilities were selected as scenarios for the measurements. These facilities are located at the Department of Mechanical and Manufacturing Engineering, Aalborg University. The first lab is an "open production space" (OPS) which consists of laboratory machinery, robots and a production line, surrounded by relatively large empty areas around the different production equipments. The second lab is a "dense factory clutter" (DFC) facility where large metallic machinery is present like metal welding machines,

hydraulic press, and material processing machines. Both labs has a similar size of approximately $35 \times 14 \times 6$ m. As it can be seen in Figures 1 and 2, which display an overview of both scenarios, the DFC represents a denser industrial clutter type than the OPS.
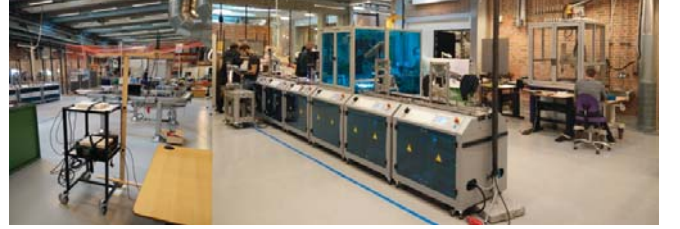

Fig. 1. View of Lab1, open production space (OPS).

Fig. 2. View of Lab2, dense factory clutter (DFC).

The measurements are performed at 24 locations which are approximately uniformly spatial-distributed over each lab facility with a minimum and maximum distance of 2 m and 34 m respectively. The measurement locations are carefully selected based on visual inspection to investigate the radio propagation in LOS (Line-of-Sight) and NLOS (Non-Line-of-Sight) conditions. In the OPS lab facility, 15% and 85% of the measurement points are classified to be in LOS and NLOS conditions respectively, while the DCF lab facility has slightly less measurement points in LOS condition (11%). During the static measurement campaign, the measurement acquisition nodes are deployed at 12 different locations and the path loss between each node antennas is estimated. Multiple redeployments of this setup are executed for each frequency to estimate the path loss between all possible combinations of the measurement locations; with this, a total of 24×23 spatial combinations considering all the different antenna configurations (higher link 1.75 m -1.75 m, lower link 0.25 m - 0.25 m, and the cross-link between the high and low antenna heights 1.75 m - 0.25 m) are estimated, resulting in 8,832 measurement links. These antenna heights were both selected below average surrounding clutter height, in order to increase the shadowing probabilities and levels in NLOS conditions as compared to clear LOS (which would have been the case of having antennas above average clutter height). By doing this we have two different references of, for example, two representative heights at which sensors or controllers in future automation systems will be deployed.
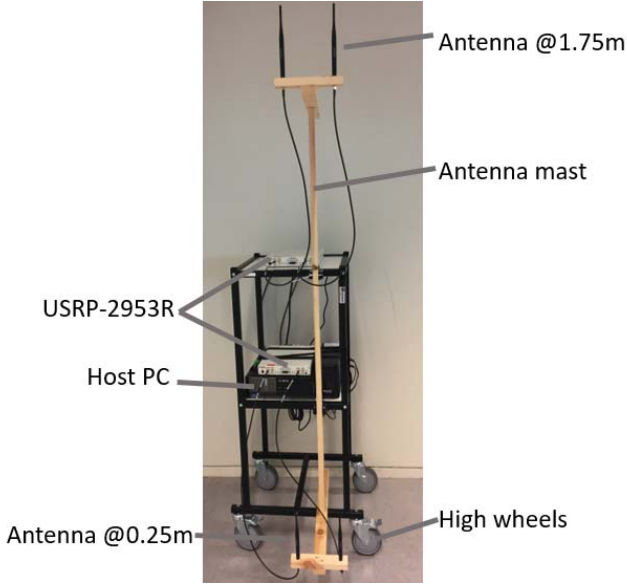
B. Measurement setup

Fig. 3. Measurement acquisition node.

The measurement setup is based on a software-defined radio (SDR) platform. Our platform is based on USRP-2953R [9] which supports synchronized transmission and reception of wireless radio signal over two radio frequency (RF) chains within the frequency range 1.2-6 GHz. A measurement acquisition node is built from two USRP boards which allow a synchronized transmission or reception of RF signal over four RF chains. Figure 3 depicts the measurement acquisition node with a support of two selected antenna heights (1.75 m and 0.25 m) and two dipole antennas mounted at each specific height. The overall testbed measurement setup consists of 12 acquisition nodes, where coordinated transmission and measurement acquisition are based on time-division multiplexing (TDM); while only one node is transmitting a reference signal with a 24 MHz bandwidth over four transmitter antennas in a time-interleaved fashion, the other nodes are simultaneously receiving and recording the signal over the four antennas. The wideband received power [1] on each antenna port is calculated for estimating the path loss between all possible 16 combinations of transmitter and receiver antennas among the nodes.

Each antenna port transmits a calibrated power of about 6 dBm and 5 dBm for 2.3 GHz and 5.7 GHz, respectively. Each of the receivers has a gain of 30 dB and the sensitivity is about -100 dBm. The antennas at both sides were similar with a peak gain of approximately 2 dBi at both frequencies. Under this particular configuration, and considering a SNR of 10 dB, the maximum measurable path loss is about 126 dB at 2.3 GHz and 125 dB at 5.7 GHz. The measurement setup has been calibrated in an outdoor open space environment within

[1]Complex channel transfer function measurements were performed so it will also possible to estimate other channel parameters such as power delay profile, however, the focus of this paper is only on large-scale propagation.

LOS conditions, where the measured path loss was verified to match with free-space path loss with a maximum deviation of ± 1.5 dB.

III. RESULTS AND DISCUSSION

Large-scale propagation refers to the received signal power attenuation (path loss) with distance where the relation can be expressed by using statistical models which capture the logarithmic distance-dependence [10]. The general formulation is given as follows:

$$PL(d) = PL(d_0) + 10\gamma log_{10}\left(\frac{d}{d_0}\right) + X_\sigma \qquad (1)$$

Where $PL(d)$ is the path loss at distance d (in m) between the transmitter and receiver in dB, $PL(d_0)$ is the intercept/reference point which is known as the mean path loss in dB at reference distance d_0 in m, γ is the path loss exponent and X_σ is a zero-mean Gaussian random variable with standard deviation σ in dB. The parameters $PL(d_0)$, γ and σ are commonly estimated by least-square fitting of measurement data using different models, such as the alpha-beta (AB) model and the close-in (CI) free-space reference distance model [10]. The main difference between the models relies on the statistical linear regression intercept; in the AB model, the intercept (known as β) is determined by the least-square fit of measurement data while in CI model the intercept is equal to the free-space path loss at a reference distance d_0= 1 m. In this work, the path loss exponent γ of AB and CI models is expressed as α and n respectively. In addition, X_σ is usually modeled as log-normal distribution, with a variability equal to the standard deviation of the residuals. The residuals are calculated from the deviations of the measurement data from the model least-square fitting; these provide an indication on the shadow fading level. We use both the AB and CI models for highlighting the large-scale propagation differences among the considered industrial scenarios, frequencies, and antenna heights.

A. Large-scale propagation measurement results and derived models

In this subsection, large-scale propagation measurement results and parameterization of the AB and CI path loss models are presented. These models are well known and widely used statistical large-scale propagation models [10]. They are also considered as a baseline for comparison of the propagation in different conditions, frequencies, and scenarios.

Figure 4 shows the measured path loss results and the least-square fitted AB model for the OPS facility at 2.3 GHz. In the figure, path loss results are categorized in LOS conditions and NLOS conditions for the different antenna configurations (higher, cross and lower links). The derived AB model for each of the cases is represented with a dashed line of a different color. As a reference, the figure also depicts the free-space path loss (FSPL) at 2.3 GHz. As it can be seen, the LOS propagation follows the free-space path loss. In addition, the figure shows that the path loss versus distance slope becomes

| Lab1, open production space (OPS)			AB Model			CI Model	
			β [dB]	α	σ [dB]	n	σ [dB]
Frequency	Conditions	Transmitter - Receiver Antenna Height Configurations					
2.3 GHz	LOS		43.1	1.6	5.1	2.0	5.2
	NLOS	1.75 m-1.75 m (higher)	46.2	1.7	6.0	2.3	6.1
		1.75 m-0.25 m (cross)	44.7	2.2	6.0	2.6	6.1
		0.25 m-0.25 m (lower)	45.0	2.4	6.2	2.9	6.3
5.7 GHz	LOS		46.2	2.0	5.6	1.9	5.6
	NLOS	1.75 m-1.75 m (higher)	48.6	2.2	7.0	2.3	7.0
		1.75 m-0.25 m (cross)	48.8	2.5	7.6	2.7	7.6
		0.25 m-0.25 m (lower)	42.5	3.4	9.1	3.0	9.2
Lab2, dense factory clutter (DFC)							
2.3 GHz	LOS		47.8	1.0	5.1	2.0	5.4
	NLOS	1.75 m-1.75 m (higher)	42.7	2.0	5.6	2.3	5.6
		1.75 m-0.25 m (cross)	42.0	2.5	6.5	2.7	6.5
		0.25 m-0.25 m (lower)	42.6	2.8	7.6	3.1	7.7
5.7 GHz	LOS		52.9	1.3	5.5	1.9	5.6
	NLOS	1.75 m-1.75 m (higher)	46.5	2.5	7.2	2.4	7.2
		1.75 m-0.25 m (cross)	47.2	2.8	8.3	2.8	8.3
		0.25 m-0.25 m (lower)	42.9	3.5	9.1	3.1	9.1
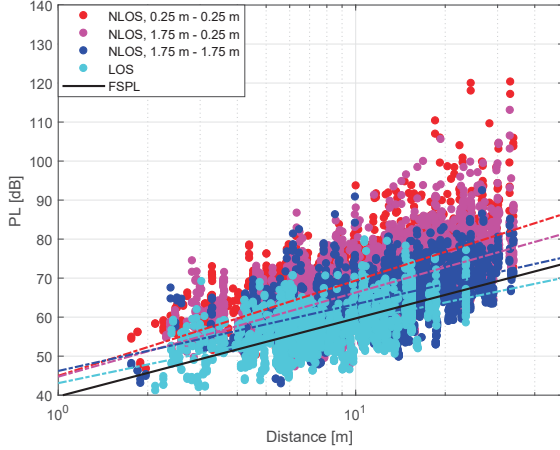
Fig. 4. Measured path loss and AB model for OPS industrial lab facility at 2.3 GHz frequency, LOS condition and NLOS condition with different antenna heights.

steeper for configurations with low antenna height. This is caused by obstacles in the propagation paths since the lower transmitter/receiver antennas are mounted 0.25 m above the floor and located clearly below the average factory equipment height as compared to the highest antenna location. Similar trends, with different numerology are observed at 5.7 GHz as compared to 2.3 GHz at both lab facilities, but we have decided not to show them explicitly as they will result in a very similar plot to Figure 4. A summary of the parametrization of all derived path loss models, considering all cases, can be found in Table I.

As it can be seen in the table, both the AB and CI models exhibit similar trends. The LOS path loss exponent of the CI model is close to the free-space path loss exponent ($n =$ 1.9 − 2.0) for both frequencies and industrial environments. However, in the AB model prediction, which is the direct fit of the measurement data, the path loss exponent is lower than free space ($\alpha = 1.0 - 2.0$). This indicates that waveguiding effects are introduced by the confined environment and the presence of many large metallic machines. Some evidence to this can be seen in the fact that the DFC environment, having more metallic machines, exhibits lower path loss exponents compared with the OPS scenario. Similar findings were also reported in [3], [5] and [8]. In NLOS condition most of the propagation paths are obstructed by the presence of factory machinery, which leads to extra losses, resulting in higher path loss exponents for both of the AB and CI modeling approaches.

The path loss exponents in NLOS conditions are clearly dependent on the antenna height; the path loss exponents are increaseing for configurations with lower transmitter/receiver antenna height. For instance, with focus on 2.3 GHz and the OPS scenario, it can be seen that the path loss exponent of the AB model (α) increases from 1.7 to 2.4 when we look at the higher and the lower link, respectively. A similar conclusion can be reached by looking at the CI model fit in the same scenario, where in this case the path loss exponent (n) increases from 2.3 to 2.9. As it was explained in connection to Figure 4, the configurations with lower antenna heights have a higher probability of propagation paths blockage and lead to larger path loss exponents as compared to the configurations with higher antenna heights, which are closer to LOS conditions. This fact also explains the larger shadow fading standard deviation (σ) for configurations with lower antenna height. For instance, and with focus on the same scenario, OPS at 2.3 GHz, the standard deviation considering the AB model increases from 6.0 dB in the higher link to 6.2 dB in the lower link. Very similar standard deviation values are observed with

both the AB and CI modeling approaches. This indicates a very similar fit in both cases.

The DFC scenario presents larger shadow fading levels as a consequence of the higher NLOS probability due to the presence of more metallic machinery as compared to the OPS scenario. This results into a higher NLOS path loss exponent and standard deviation. For 2.3 GHz, the path loss exponents (α) in the DFC scenario are in the range 2-2.8 (as compared to the 1.7-2.4 in the OPS), and the standard deviation is up to 1.4 dB larger than in the OPS scenario.

By looking at the frequency dependency, the path loss exponents and shadow fading standard deviation increase when the frequency increases from 2.3 GHz to 5.7 GHz for both LOS and NLOS conditions. On the other hand, the work in [5] reported that the path loss exponent and shadow fading standard deviation decrease with increasing frequency. These can be explained by the antenna height difference; in [5] the transmitter and receiver antenna height were mounted in 6 m and 2 m above the floor respectively, this transmitter antenna height is far above the height of the large metallic machinery, whereas in our setup the transmitter and receiver are mounted 1.75 m or 0.25 m above the ground whose heights are comparable with the height of the large machines or below. Because of this height difference, our NLOS scenario seems to be driven by diffraction and blockage, while the scenario in [5] seems to driven by reflection due to the elevated transmitter height clearly above the average machinery clutter height.

In perspective of exploring the challenge related to achieving higher levels of reliability, it is worth to be mentioned that the worst propagation conditions are observed in the DFC with a maximum mean path loss exponent of up to 2.8 and 3.5 for 2.3 and 5.7 GHz, respectively. In terms of shadow fading standard deviation, the maximum observed values are 7.6 dB at 2.3 GHz and 9.1 dB at 5.7 GHz.

B. Measurement results in perspective of ultra-reliable communication

In order to remove cable connections in industrial scenarios and replace them with 5G wireless units, very stringent requirements in terms of maximum packet error rate (10^{-5}) and latency (1 ms) should be met [1]. Regarding that matter, the work in [11] indicated that to provide such ultra-reliable communication, the focus should be on the behavior of the channel at a probabilities of 10^{-5} or less in the signal reception. These probabilities reflect the occurrence of rare events which may have significant impact on the radio signal availability, and thus in the reliability in a given scenario. Based on that argumentation, any channel model used in the design and evaluation of 5G ultra-reliable systems should be derived or validated based on well planned and extensive measurement data sets, containing enough representative information of the propagation in the scenario to capture the occurrence of those rare events.

Following the previous premises, we try to illustrate and highlight the impact of such rare events in the ultra-reliability
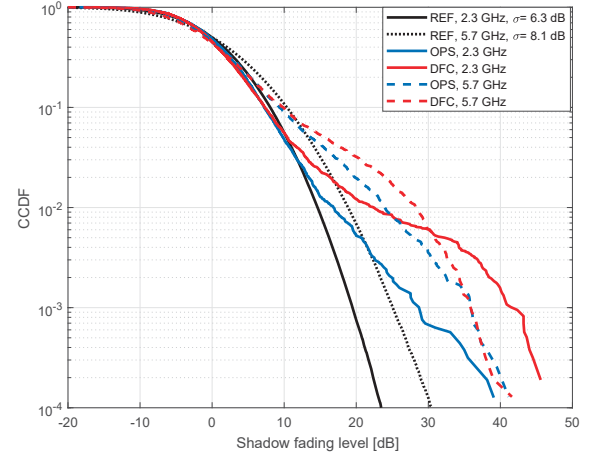

Fig. 5. Complementary cumulative distribution function of the measured shadow fading level in both the OPS and DFC facilities for both frequencies.

regime, by analyzing the shadow fading distributions extrapolated from our measurements. Figure 5 depicts the complementary cumulative distribution function (CCDF) of the empirical shadow fading distributions, considering all the LOS and NLOS samples and all the different antenna configurations, computed over the AB model for both the OPS and DFC scenarios at 2.3 and 5.7 GHz. As a reference for the analysis, the figure also displays a theoretical reference based on the model in (1), in which the common assumption of log-normal shadow fading has been applied with average NLOS standard deviation (6.1 dB at 2.3 GHz and 8.3 dB at 5.7 GHz). As it can be seen, the different empirical OPS and DFC distributions follow closely the log-normal reference distribution, with deviations smaller than 1 dB up to levels of approximately 10^{-1} (90% of availability). Below that probability, large-scale fading levels deviate considerably from the assumed model, despite being parametrized with the same standard deviation. This deviation is as large as 20 dB at the 10^{-3} percentile (observed at 2.3 GHz in the DFC scenario) and larger for lower percentiles (24 dB close to the 10^{-4} percentile 99.99% of availability).

Further, the empirical shadow fading distributions show that the scenario (clutter type) has a larger impact at 2.3 GHz than at 5.7 GHz. In the DFC the shadowing can be as severe as 46 dB close to the 10^{-4} level while the OPS is approximately 8 dB better. For the same probability level, at 5.7 GHz, both the OPS and DFC exhibit a similar shadowing level of approximately 40 dB. The same conclusion can be reached by looking at the overall distribution trends, where it is clearly visible that both the OPS and DFC distributions are very similar at 5.7 GHz. On the other hand, at 2.3 GHz, the DFC distribution presents larger shadowing levels than the OPS distribution. A possible explanation for the observed trends can be that, in the industrial scenarios, at 2.3 GHz, diffraction is dominant over other propagation mechanisms, which translates

into larger losses for larger NLOS probabilities, and thus a larger loss in the DFC as compared to the OPS. Differently, at 5.7 GHz, other propagation mechanisms may have relatively larger impact, e.g. reflection (and scattering) losses, to reduce the difference between the two clutter types.

One can speculate that the deviations from the log-normal reference will continue to increase for even lower outage probabilities like the targeted 10^{-5} which should set the margin for the planning of ultra-reliable systems. Experimentally verifying this is proven to be difficult. Despite our measurement effort to collect a large number of spatially distributed samples, further work is needed to make accurate predictions on the lower tail of the distribution.

C. Point-cloud simulations as a complement to the measurements

In order to extend further the statistics from measurements and to characterize the environment with higher resolution, we are exploring the feasibility of basing the analysis on deterministic field predictions built on point-cloud methods [12]. These ray-tracing techniques use as an input detailed maps of the environment rather than simplified geometrical descriptions of it. These maps are based on the laser scan of the physical environment, and take the shape of a cloud of points representing the different interaction points of the laser ray with the obstacles present in the environment. Based on this cloud of points, it is possible to simulate the propagation between two locations inside the scenario by considering these points of interaction as potential sources of diffraction, reflection or scattering. The simulation will be calibrated by using a subset of the measurements, while another will be kept for verification. From the calibrated predictions, we expect to be able to match the channel statistics for the higher percentiles, getting more detailed insight onto the lower tails. The advantage of using such prediction methods is the possibility of running "virtual" measurement campaigns over a much larger number of locations, situations, or link combinations than in a real-world measurement campaign.

IV. CONCLUSIONS

This paper presented the results and analysis of wideband large-scale propagation based on extensive measurements performed in two different industrial scenarios (open production space and dense factory clutter) at 2.3 GHz and 5.7 GHz. The measurements were conducted over a total of 24 uniformly spatial-distributed locations in each of the labs, considering multiple antenna configurations at 0.25 and 1.75 m heights. The results show that in both scenarios, the path loss exponents (α) are below 2 in LOS, due to the waveguiding effects caused by multiple reflections on the many metallic machines. In NLOS conditions, the path loss exponents increase for lower antenna heights, reaching values of up to 2.4 and 3.4 at 2.3 and 5.7 GHz, respectively, in the open production space. This values are larger in the dense factory clutter, reaching values of 2.8 at 2.3 GHz and 3.5 at 5.7 GHz. The same increasing trend with lower antenna heights is observed for the shadow

fading standard deviations (σ). In this case, the maximum values at 2.3 GHz and 5.7 GHz are, respectively, 6.2 and 9.1 dB and in the open production space and 7.6 and 9.1 dB in the dense factory clutter. From the analysis of the lower percentiles of the shadow fading distributions, it is possible to see that the shadow fading levels can be as severe as 38-46 dB at 2.3 GHz, and approximately 40 dB at 5.7 GHz, close to the 10^{-4} level (99.99% of spatial availability). It is also possible to see that the commonly applied log-normal distributions fail to predict for probabilities lower than 10^{-1}, finding deviations of up to 20 dB for that low percentiles. It is expected that further insight on lower percentiles will be achieved by exploiting the ability of running much more extensive virtual measurement campaigns by means of advanced calibrated simulation methods.

REFERENCES

[1] 3GPP TR 38.913 v14.1.0, Study on Scenarios and Requirements for Next Generation Access Technologies, Mar. 2017.

[2] T. S. Rappaport and C. D. McGillem, "UHF fading in factories," in IEEE Journal on Selected Areas in Communications, vol. 7, no. 1, pp. 40-48, Jan. 1989.

[3] S. Kjesbu and T. Brunsvik, "Radiowave propagation in industrial environments," 2000 26th Annual Conference of the IEEE Industrial Electronics Society. IECON 2000. 2000 IEEE International Conference on Industrial Electronics, Control and Instrumentation. 21st Century Technologies, Nagoya, 2000, pp. 2425-2430 vol.4.

[4] H. Farhat, L. Minghini, J. Keignart and R. D'Errico, "Radio channel characterization at 2.4 GHz in nuclear plant environment," 2015 9th European Conference on Antennas and Propagation (EuCAP), Lisbon, 2015, pp. 1-3.

[5] E. Tanghe et al., "The industrial indoor channel: large-scale and temporal fading at 900, 2400, and 5200 MHz," in IEEE Transactions on Wireless Communications, vol. 7, no. 7, pp. 2740-2751, July 2008.

[6] C. B. Andrade and R. P. Fabris Hoefel. On Indoor Coverage Models for Industrial Facilities. 7th international telecommunication symposium (ITS2010).

[7] J. Ferrer-Coll, P. Angskog, J. Chilo and P. Stenumgaard, "Characterisation of highly absorbent and highly reflective radio wave propagation environments in industrial applications," in IET Communications, vol. 6, no. 15, pp. 2404-2412, October 16 2012.

[8] S. Phaiboon,"Space diversity path loss in modern factory at frequency of 2.4GHz,"in WSEAS transactions on communications, vol. 13, 2014.

[9] National Instruments USRP-2953R [Online], 2017. Available: http://www.ni.com/da-dk/support/model.usrp-2953.html

[10] M. Peter, W. Keusgen and R. J. Weiler, "On path loss measurement and modeling for millimeter-wave 5G," 2015 9th European Conference on Antennas and Propagation (EuCAP), Lisbon, 2015, pp. 1-5.

[11] P. C. F. Eggers and P. Popovski,"Wireless channel modeling perspectives for ultra-reliable commnications," [Online], 2017. Available: http://arxiv.org/abs/1705.01725

[12] J. Jarvelainen, K. Haneda and A. Karttunen, "Indoor Propagation Channel Simulations at 60 GHz Using Point Cloud Data," in IEEE Transactions on Antennas and Propagation, vol. 64, no. 10, pp. 4457-4467, Oct. 2016.